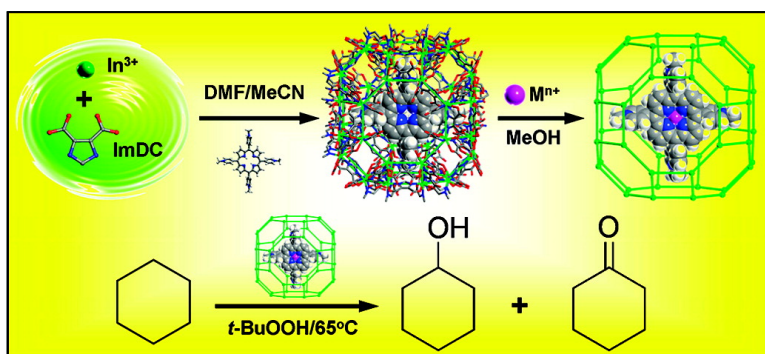


Zeolite-like Metal#Organic Frameworks as Platforms for Applications: On Metalloporphyrin-Based Catalysts

Mohamed H. Alkordi, Yunling Liu, Randy W. Larsen, Jarrod F. Eubank, and Mohamed Eddaoudi
J. Am. Chem. Soc., **2008**, 130 (38), 12639-12641 • DOI: 10.1021/ja804703w • Publication Date (Web): 29 August 2008

Downloaded from <http://pubs.acs.org> on February 8, 2009



More About This Article

Additional resources and features associated with this article are available within the HTML version:

- Supporting Information
- Links to the 2 articles that cite this article, as of the time of this article download
- Access to high resolution figures
- Links to articles and content related to this article
- Copyright permission to reproduce figures and/or text from this article

[View the Full Text HTML](#)

Zeolite-like Metal–Organic Frameworks as Platforms for Applications: On Metalloporphyrin-Based Catalysts

Mohamed H. Alkordi, Yunling Liu,[†] Randy W. Larsen, Jarrod F. Eubank, and Mohamed Eddaoudi*

Department of Chemistry, University of South Florida, 4202 East Fowler Avenue (CHE205), Tampa, Florida 33620

Received June 19, 2008; E-mail: eddaoudi@cas.usf.edu

Metal-organic frameworks (MOFs) have emerged as a particular class of functional solid-state materials owing to their unique attributes, crystalline open structures with periodic dual composition amenable to bottom-up assembly of judiciously designed molecular building blocks into a desired framework expanding and/or decorating a specific blueprint network topology.¹ These features have permitted the assembly of open functional MOFs with modular compositions and tailorable pores and hence offer great potential to address some key applications such as hydrogen storage, carbon dioxide sequestration, enhanced catalysis, smart sensors, and drug delivery.²

A major impetus to advance MOF applications is the development of new pathways and strategies to construct made-to-order MOFs as platforms suitable for a desired application. Toward this effort, we developed a new approach for construction of MOFs based on the assembly of rigid and directional single-metal-ion-based molecular building blocks (MBBs).³ This approach has spawned the construction of a new subclass of MOFs, namely zeolite-like metal–organic frameworks (ZMOFs), based on the assembly of rigid and directional InN_4 tetrahedral building units (TBUs). ZMOFs are topologically analogous to pure inorganic zeolites and, similarly, are anionic and chemically stable in aqueous media, atypical in common MOFs. Additionally, ZMOFs possess extra-large cavities, which offer great potential for their exploration in applications pertinent to larger molecules. Here we present the use of a ZMOF as a platform to anchor and isolate catalytically active metalloporphyrins, prohibiting their self-dimerization and oxidative degradation, which allows enhancement of their catalytic properties.

Metalloporphyrins have widespread applications in catalytic oxidation, for example, hydroxylation and epoxidation of hydrocarbons.⁴ Nevertheless many homogeneous metalloporphyrin-based catalysts suffer from limited lifetime activity due to the formation of bridged μ -oxide dimers (hindered access to catalytic sites) and oxidative self-degradation.⁵ Therefore, immobilization of metalloporphyrins in solid matrices provides a promising approach to overcome such drawbacks,⁶ where the macrocycle can be isolated and its catalytic site protected. Modified mixed oxide surfaces⁷ and porous inorganic solids (i.e., zeolites X and Y,⁸ mesoporous silicates,⁹ silica surfaces¹⁰) have been investigated as solid-state matrices to immobilize metalloporphyrins; however, these systems also are faced with limitations, including aggregation of the catalyst molecules, limited catalyst loadings resulting in potential non-periodic distribution, and/or leaching of the catalyst.

A suitable host matrix must possess several attributes: (i) large cavities, suitable for the encapsulation of one guest porphyrin molecule per cavity, with relatively reduced openings that prevent catalyst leaching while allowing diffusion of reactants and products;

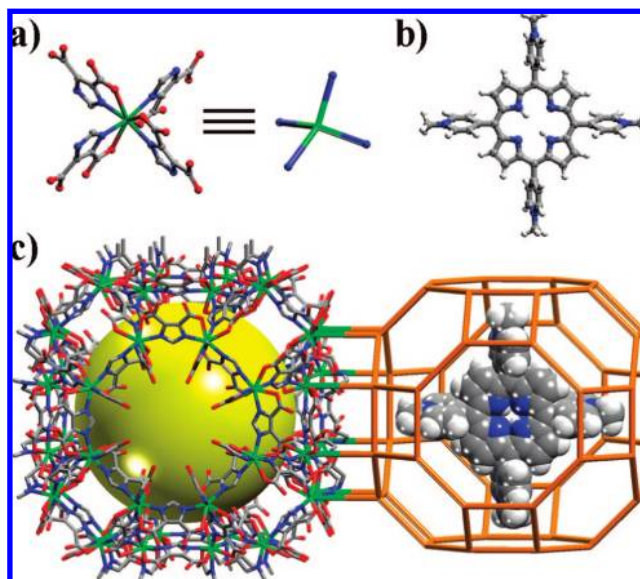


Figure 1. (a) Eight-coordinate MBB that could be represented as a TBU, (b) $[\text{H}_2\text{TMPyP}]^{4+}$ porphyrin, (c) crystal structure of *rho*-ZMOF (left), hydrogen atoms omitted for clarity, and schematic presentation of $[\text{H}_2\text{TMPyP}]^{4+}$ porphyrin ring enclosed in *rho*-ZMOF α -cage (right, drawn to scale).

(ii) mild synthesis conditions and the presence of framework-porphyrin directing interactions, for example, electrostatics, permitting the one-step framework construction and encapsulation of the free-base porphyrin; (iii) maintained framework integrity upon postsynthesis metalation of the encapsulated porphyrin (e.g., framework stability in aqueous media) and under the investigated catalytic oxidation conditions; (iv) low affinity for the oxidation products, thus allowing for their diffusion into the bulk solution and ease of separation (e.g., filtration) from the heterogeneous catalyst. In fact, our recently synthesized (indium-imidazoledicarboxylate)-based *rho*-ZMOF (topologically analogous to zeolite RHO) offers great potential to answer such criteria and serves to simultaneously merge the realms of MOFs and zeolites with the catalytic properties of porphyrins to forge a unique tunable catalyst platform. The large voids inside its periodic α -cages and their anionic nature suggest the ability for encapsulation of cationic porphyrins. Indeed, reactions of $\text{In}(\text{NO}_3)_3 \cdot x\text{H}_2\text{O}$ and 4,5-imidazoledicarboxylic acid (H_3ImDC) in an *N,N'*-dimethylformamide (DMF)/acetonitrile (CH_3CN) mixture in the presence of 5,10,15,20-tetrakis(1-methyl-4-pyridinio)porphyrin tetra(*p*-toluenesulfonate) ($[\text{H}_2\text{TMPyP}] [p\text{-tosyl}]_4$) have yielded dark red cubic-like crystals, suggesting the presence of the porphyrin, Figure 1.¹¹ The crystals, insoluble in water and common organic solvents, were washed with DMF and methanol several times, until no residual porphyrin was detected in the solution, as evident from the UV–vis spectrum. The powder X-ray diffraction (PXRD) pattern of the as-synthesized

[†] Present address: State Key Laboratory of Inorganic Synthesis and Preparative Chemistry, Jilin University, Changchun 130012, P. R. China.

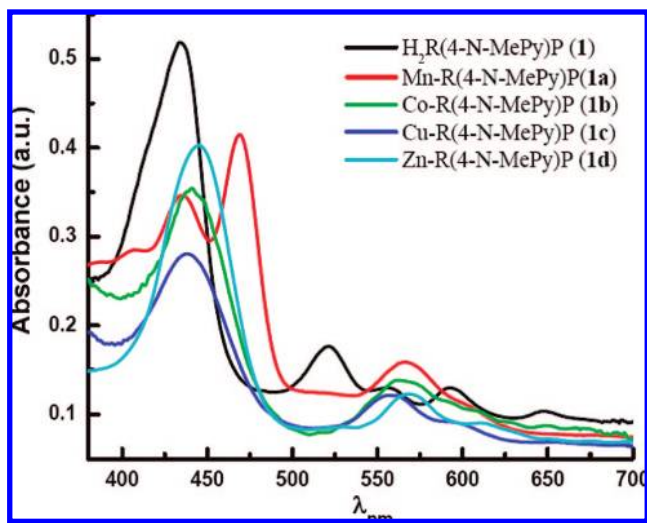


Figure 2. Diffuse-reflectance, solid-state UV-vis spectra of **1** and its various metalation products (**1a–d**).

compound matches that of our previously published colorless *rho*-ZMOF³ (Supporting Information), confirming the construction of the intended crystalline framework; the structure is further supported by single-crystal studies, which confirm identical crystallographic parameters to *rho*-ZMOF (cubic, $Im\bar{3}m$, $a = 31.0622(7)$ Å). The framework structure is based on 8-coordinate In^{3+} ions N-, O-heterochelated by four separate HImDC ligands ($In_4(CO_2)_4$ MBB) to give In_4 TBUs. The assembly of the 4-connected TBUs results in the generation of truncated cuboctahedra (the α -cage is enclosed by 48 In_4 TBUs), which link together through double eight-member rings (D8R) to form the *rho*-ZMOF. The framework unit cell (volume eight times larger than conventional inorganic zeolite RHO) is formulated as $([In_{48}(HImDC)_{96}]^{48-})$, where the negatively charged framework is balanced by cationic guest molecules.

The presence of $[H_2TMPyP]^{4+}$ was confirmed by solid-state UV-vis studies of the fully washed crystalline solid, $H_2RTMPyP$ (H_2TMPyP encapsulated in *rho*-ZMOF, R) (**1**), where the spectrum shows the characteristic five absorption bands associated with the free-base porphyrin ($\lambda_{max} = 434, 522, 556, 593, 648$ nm), Figure 2. Accordingly, the porphyrin was not metallated by In^{3+} present in the assembly conditions. It should be noted that the inclusion of the porphyrin inside the cages of *rho*-ZMOF could not be verified by single-crystal XRD due to the lower symmetry of the porphyrin molecules, C_1 , compared to the cubic $Im\bar{3}m$ symmetry of the framework, that is, not enough constraints can be exerted on the multiple possible orientations of the porphyrin molecule inside the cages, believed to be necessary to induce long-range order inside *rho*-ZMOF.

Incubation of **1** in an aqueous solution of Na^+ ions showed no release of the porphyrin, as indicated by UV-vis studies of the solution. In contrast, smaller cationic molecules, such as acridines, can be reversibly immobilized (through electrostatic interactions) inside *rho*-ZMOF cavities through ionic exchange due to their smaller dimensions, ca. less than 1 nm.³ Dissolving **1** under strongly acidic conditions allows release of the porphyrin into solution, which permits the estimation of the loaded amount of $[H_2TMPyP]^{4+}$ to be 2.5 wt %, controllable via variable concentration of free-base porphyrin during synthesis of **1**.¹² These findings prove the encapsulation of the free-base porphyrin, and support the absence of porphyrin leaching, mainly due to the relatively smaller size of the window openings to the α -cages, that is, D8Rs. In addition,

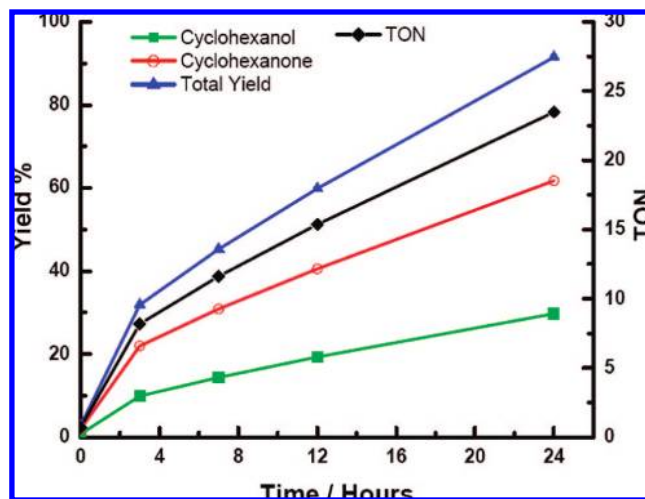


Figure 3. Cyclohexane catalytic oxidation using **1a** as a catalyst at 65 °C. Yield % based on TBHP, 1 equiv consumed per alcohol produced and 2 equiv consumed per ketone produced.

similar in situ encapsulation conditions to the aforementioned cationic porphyrin did not permit the encapsulation of neutral nor anionic porphyrins nor phthalocyanines inside *rho*-ZMOF, supporting the importance of electrostatic interactions between the cationic porphyrin and the anionic framework during the simultaneous self-assembly and encapsulation processes.

Potential metalation of the free-base porphyrin $H_2RTMPyP$, **1**, will allow for its utilization and exploration as a platform for metalloporphyrin-based catalysis. Indeed, we have successfully metallated the encapsulated free-base porphyrin, postsynthesis, by exposing **1** to various solutions of transition metal ions. Metalation of **1** by various transition metal cations was accomplished via incubation of **1** in a 0.1 M methanol solution of the corresponding metal nitrate at room temperature for up to 24 h. The crystals were subsequently washed with H_2O and methanol several times and air-dried at 40 °C. The expected metalation was confirmed by UV-vis studies as indicated by the red-shifted Soret-bands and collapse of the Q-bands multiplets upon metalation, Figure 2. Crystals of **1** yield M-RTMPyP, after metalation, where M = Mn, Cu, Zn, or Co ions (**1a**, **1b**, **1c**, **1d**, respectively).

To assess catalytic activity, hydrocarbon oxidation was performed in the presence of Mn-RTMPyP, **1a**. Specifically, the crystalline solid **1a** was explored as a catalyst for cyclohexane oxidation. Under neat conditions, the oxidation was performed at 65 °C in the presence of *tert*-butyl hydroperoxide (TBHP) as the oxidant, chlorobenzene as an internal standard, and **1a** as the catalyst;¹³ the reaction progress was monitored by analyzing aliquots of the bulk solution using GC-FID. After 24 h, based on the amount of oxidant present in the initial reaction mixture, a total yield (from cyclohexane to cyclohexanol/cyclohexanone) of 91.5% and a corresponding turn over number (TON) of 23.5 (catalyst loading of 3.8%) were observed (Figure 3) a noticeably higher yield compared to other systems of supported metalloporphyrins (zeolites or mesoporous silicates) (Supporting Information, Table S1). The reaction products were formed in almost stoichiometric amounts. The yield % was calculated assuming a 2:1 TBHP to cyclohexane molar ratio, necessary to produce cyclohexanone through oxidation of the intermediate cyclohexanol.

The weakly polar hydrocarbon products should have low affinity for the highly polar *rho*-ZMOF framework and thus readily diffuse into the solution. Cyclohexanol and cyclohexanone were the only observed products, identified through their retention times compared

to authentic samples, suggesting that the investigated oxidation reaction is selective toward the formation of this alcohol and ketone under the conditions employed (i.e., no further oxidation products were detected).

The solid matrix **1a** readily can be separated from the product solution by simple filtration, a feature unique to heterogeneous solid-immobilized catalysts that allows for studies of recyclability of the catalyst/platform. Indeed, **1a** is recyclable under the reaction conditions up to at least the 11th cycle (the reported results in this study), as **1a** retains its crystallinity, reactivity, and selectivity throughout this number of cycles. Each cycle was run for 24 h, and then **1a** was isolated, washed with methanol, and dried at 40 °C. No leaching of the encapsulated metalloporphyrin was observed as evident from the UV–vis spectrum of the product solution. In fact, catalytic activity was observed only when crystals of **1a** were present in the reaction mixture. No catalytic activity was observed for the control reactions: (1) in the absence of porphyrin and *rho*-ZMOF, (2) in the presence of only the *rho*-ZMOF (no porphyrin), (3) in the presence of Mn²⁺-exchanged *rho*-ZMOF (no porphyrin), and (4) in the presence of **1** (free-base porphyrin in *rho*-ZMOF). These results confirm that the observed catalytic behavior is unique to **1a**, *rho*-ZMOF impregnated with Mn-metallated porphyrin.

Here we have demonstrated the utilization of our (In-HImDC)-based *rho*-ZMOF as a host for large catalytically active molecules, specifically metalloporphyrins, and its effect on the enhancement of catalytic activity. To produce a versatile platform (i.e., can be tailored to meet specific applications), we encapsulated the free-base porphyrin, which was readily metallated, postsynthesis, by various transition metal ions to produce a wide range of encapsulated metalloporphyrins. Work is in progress to explore further potential of these encapsulated metalloporphyrins, including other catalytic transformations like cyclopropanation and epoxidation of alkenes. In addition, potential modifications to the encapsulated porphyrin to induce stereoselectivity and to enhance regioselectivity and/or reactivity are being investigated. Work is underway to expand this approach to other cationic molecules, which can permit access to novel functional materials suitable for catalysis, sensing, etc.

Acknowledgment. We would like to dedicate this paper to professor John D. Roberts on the event of his 90th birthday. We gratefully acknowledge the financial support of the University of South Florida and the National Science Foundation (grant DMR-0548117, M.E.), as well as ACS-PRF (grant 4323-AC4, R.W.L.). Special thanks to Dr. Roman Manetsch for helpful discussions and providing the GC-FID.

Supporting Information Available: PXRD data and catalysis comparison table. This material is available free of charge via the Internet at <http://pubs.acs.org>.

References

- (1) (a) Eddaoudi, M.; Moler, D. B.; Li, H.; Chen, B.; Reineke, T. M.; O'Keeffe, M.; Yaghi, O. M. *Acc. Chem. Res.* **2001**, *34*, 319–330. (b) Eddaoudi, M.; Kim, J.; Rosi, N.; Vodak, D.; Wachter, J.; O'Keeffe, M.; Yaghi, O. M. *Science* **2002**, *295*, 469–472. (c) Férey, G.; Mellot-Drazniak, C.; Serre, C.; Millange, F. *Acc. Chem. Res.* **2005**, *38*, 217–225. (d) Moulton, B.; Zaworotko, M. J. *Chem. Rev.* **2001**, *101*, 1629–1658. (e) Kitagawa, S.; Kitaura, R.; Noro, S.-I. *Angew. Chem., Int. Ed.* **2004**, *43*, 2334–2375.
- (2) (a) Rowsell, J. L. C.; Yaghi, O. M. *J. Am. Chem. Soc.* **2006**, *128*, 1304–1315. (b) Dinca, M.; Han, W. S.; Liu, Y.; Dailly, A.; Brown, C. M.; Long, J. R. *Angew. Chem., Int. Ed.* **2007**, *46*, 1419–1422. (c) Mulfort, K. L.; Hupp, J. T. *J. Am. Chem. Soc.* **2007**, *129*, 9604–9605. (d) Liu, Y.; Eubank, J. F.; Cairns, A. J.; Eckert, J.; Kravtsov, V. Ch.; Luebke, R.; Eddaoudi, M. *Angew. Chem., Int. Ed.* **2007**, *46*, 3278–3283. (e) Hayashi, H.; Cote, A. P.; Furukawa, H.; O'Keeffe, M.; Yaghi, O. M. *Nat. Mater.* **2007**, *6*, 501–506. (f) Llewellyn, P. L.; Bourrelly, S.; Serre, C.; Vimont, A.; Daturi, M.; Hamon, L.; DeWeireld, G.; Chang, J.; Hong, D.; Hwang, Y. K.; Jung, S. H.; Férey, G. *Langmuir* **2008**, *24*, 7245–7250. (g) Banerjee, R.; Phan, A.; Wang, B.; Knobler, C.; Furukawa, H.; O'Keeffe, M.; Yaghi, O. M. *Science* **2008**, *319*, 939–943. (h) Cho, S.-H.; Gadzikwa, T.; Afshari, M.; Nguyen, SonBinh, T.; Hupp, T. J. *Eur. Jour. Inorg. Chem.* **2007**, 4863–4867. (i) Horcajada, P.; Serre, C.; Vallet-Regí, M.; Sebban, M.; Taulelle, F.; Férey, G. *Angew. Chem., Int. Ed.* **2006**, *45*, 5974–5978.
- (3) Liu, Y.; Kravtsov, V.; Larsen, R.; Eddaoudi, M. *Chem. Commun.* **2006**, 1488–1490.
- (4) (a) Sheldon, R. A.; Kochi, J. K. *Metal-Catalyzed Oxidations of Organic Compounds*; Academic Press: New York, 1981. (b) *Metalloporphyrins in Catalytic Oxidations*; Sheldon, R. A., Ed.; Marcel Dekker: New York, 1994. (c) Collman, J. P.; Zhang, X.; Lee, V. J.; Uffelman, E. S.; Brauman, J. I. *Science* **1993**, *261*, 1404–1411. (d) *Comprehensive Supramolecular Chemistry*; Suslick, K. S., Ed.; Supramolecular Reactivity and Transport: Bioinorganic Systems; Pergamon: Oxford, 1996; Vol. 5. (e) Meunier, B. In *Metalloporphyrin Catalyzed Oxidations*; Montanari, F.; Casella, L. Eds.; Kluwer: Dordrecht, The Netherlands, 1994; pp 1–48.
- (5) Guo, C.; Song, J.; Chen, X.; Jiang, G. *J. Mol. Catal. A* **2000**, *157*, 31–40.
- (6) (a) Sacco, H. C.; Iamamoto, Y.; Lindsay Smith, J. R. *J. Chem. Soc., Perkin Trans.* **2001**, *2*, 181–190. (b) Vinhadó, F. S.; Prado-Manso, C. M. C.; Sacco, H. C.; Iamamoto, Y. *J. Mol. Catal. A* **2001**, *174*, 279–288. (c) Deniaud, D.; Spyroullias, G. A.; Bartoli, J. F.; Battioni, P.; Mansuy, D.; Pinel, C.; Odobel, F.; Bujoli, B. *New J. Chem.* **1998**, *22*, 901–905. (d) Li, Z.; Xia, C. G.; Zhang, X. M. *J. Mol. Catal. A* **2002**, *185*, 47–56.
- (7) Cardoso, S. W.; Francisco, M. P.; Landers, R.; Gushikem, Y. *Electrochim. Acta* **2005**, *50*, 4378–4384.
- (8) (a) Khan, T. A.; Hriljac, J. A. *Inorg. Chim. Acta* **1999**, *294*, 179–182. (b) Rosa, I. L. V.; Manso, C. M. C. P.; Serra, O. A.; Iamamoto, Y. *J. Mol. Catal. A* **2000**, *160*, 199–208. (c) Skrobot, F. C.; Rosa, I. L. V.; Marques, A. P. A.; Martins, P. R.; Rocha, J.; Valente, A. A.; Iamamoto, Y. *J. Mol. Catal. A* **2005**, *237*, 86–92.
- (9) (a) Xu, W.; Guo, H.; Akins, D. L. *J. Phys. Chem. B* **2001**, *105*, 1543–1546. (b) Nur, H.; Hamid, H.; Endud, S.; Hamdan, H.; Ramli, Z. *Mater. Chem. Phys.* **2006**, *96*, 337–342.
- (10) Moreira, M. S. M.; Martins, P. R.; Curi, R. B.; Nascimento, O. R.; Iamamoto, Y. *J. Mol. Catal. A* **2005**, *233*, 73–81.
- (11) All chemicals were Aldrich reagent grade and used as received, unless otherwise noted. In a 20 mL vial, a mixture of In(NO₃)₃·xH₂O (0.015 g, 0.0435 mmol), 4,5-H₂ImDC (0.014 g, 0.087 mmol), DMF (1 mL), CH₃CN (1 mL), and 0.1 mL of 8 mM methanol solution of [H₂TMPyP][p-tosyl]₄ were mixed; the vial was sealed and heated to 85 °C for 12 h, then to 105 °C for 24 h with a heating rate of 1.5 °C/min, and then cooled down to room temperature with a cooling rate of 1 °C/min. Dark red crystals of **1**, [H₂TMPyP]⁴⁺ encapsulated inside *rho*-ZMOF, were then collected, washed with DMF, and then washed with methanol several times, until no residual amount of porphyrin was present in the washing solution, as evident from the UV–vis spectrum of the washing solution.
- (12) In an attempt to maximize porphyrin loading into *rho*-ZMOF, 1.198 mmole of 4,5-H₂ImDC, 0.5 mmole of In(NO₃)₃·xH₂O, 30 μmol of [H₂TMPyP][p-tosyl]₄, DMF, and ethanol (3 mL each) were mixed in a 25 mL scintillation vial. The vial was then heated using the same procedure for the synthesis of **1**. The resultant crystals, **1'**, were washed several times with methanol until no residual porphyrin was present. A 10.8 mg portion of **1'** was dissolved in 25 mL of concd HNO₃, from which 1 mL was diluted to the volume of 10 mL using DI water. Using atomic absorption to determine concentration of In³⁺ ions and UV–vis for porphyrin (ε₄₃₈ = 1.9 × 10⁵ M⁻¹ cm⁻¹), an estimate of 67% loading of porphyrin into the α-cages (each made of 24 In³⁺ ions) was possible. Further increase of the free-base porphyrin concentration in the reaction mixture precludes formation of crystalline material.
- (13) Oxidation reaction conditions: 77 μmol TBHP, dried over MgSO₄, 100 μmol chlorobenzene as internal standard, 10 mL cyclohexane, and 88 mg of **1a** (equivalent to 2.9 μmol of Mn-TMPyP) were mixed, under aerobic conditions, in a 25 mL round-bottom flask fitted with a silicone septum. The reaction mixture was then held at 65 °C in an isothermal bath for the required amount of time, as determined by analyzing aliquots of the mixture over time using GC-FID.

JA804703W